Supplementary material

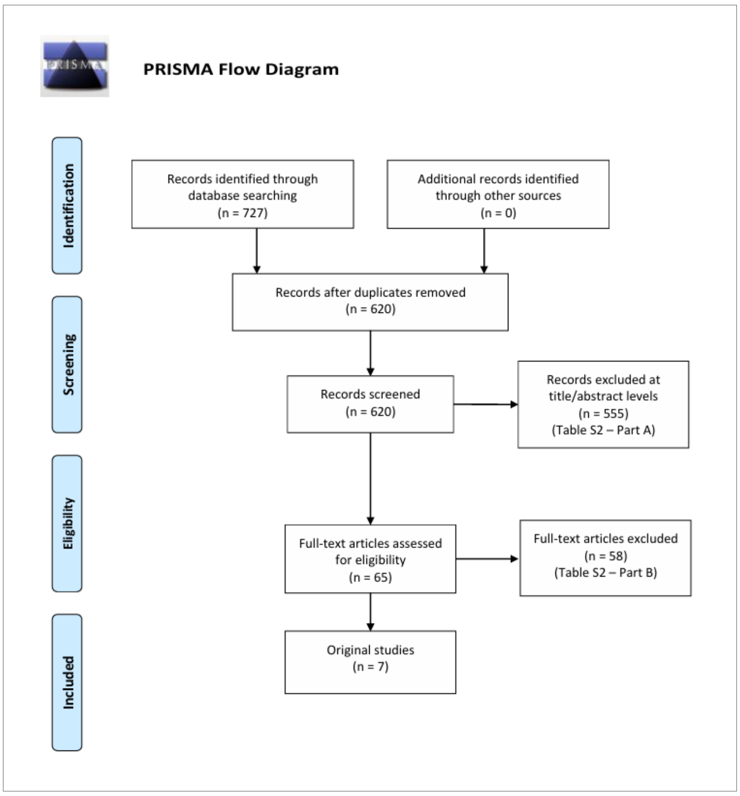

Supplementary Figure 1 Preferred Reporting Items for Systematic Reviews and Meta-Analyses flow chart.

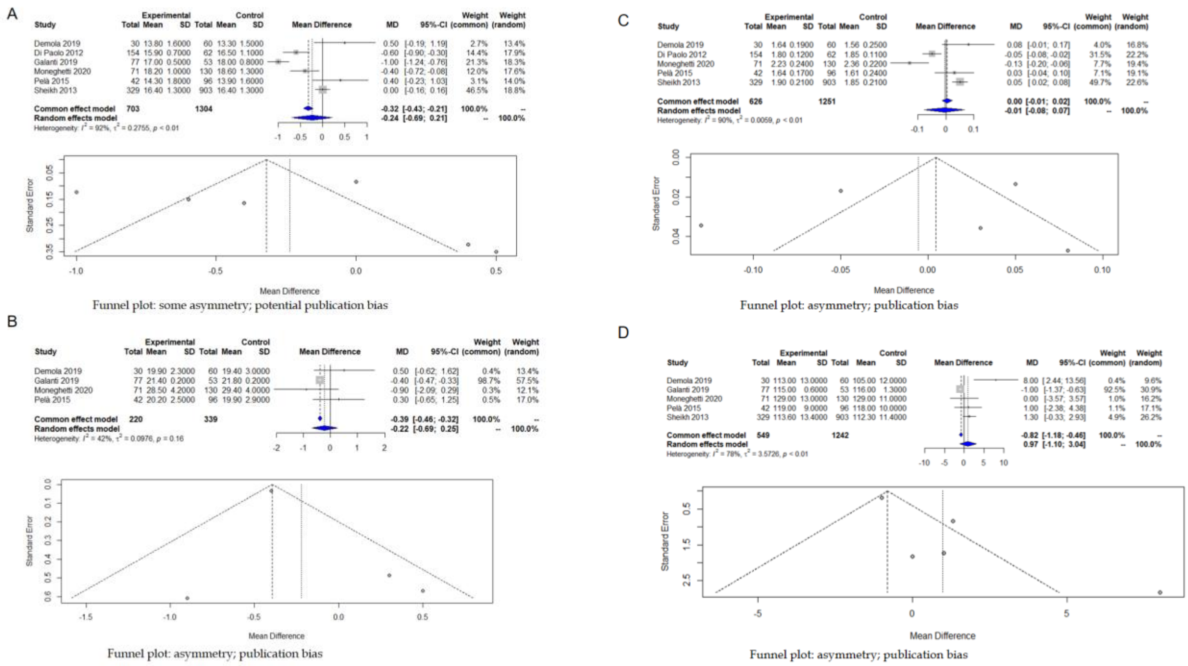

E

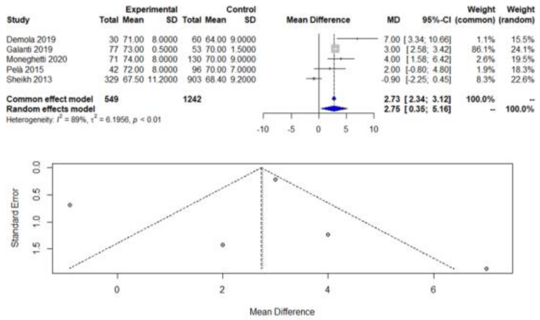

Funnel plot: some asymmetry; potential publication bias

F

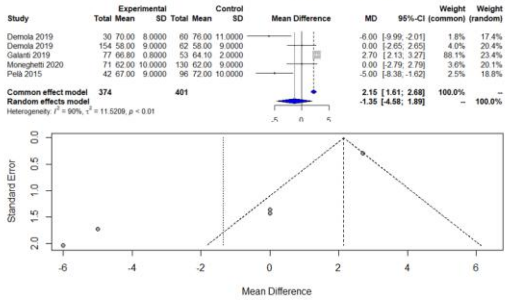

Funnel plot: asymmetry; publication bias

Supplementary Figure 2 Baseline characteristics. A: Forest and funnel plots for age. Mean difference (MD) = -0.24, 95%CI: -0.69 to 0.21, P = 0.3031; I^2 = 92%; B: Forest and funnel plots for body mass index. MD = -0.22, 95%CI: -0.69 to 0.25, P = 0.3542; I^2 =42%; C: Forest and funnel plots for body surface area. MD = -0.01, 95%CI: -0.08 to 0.07, P = 0.8754; I^2 = 90%; D: Forest and funnel plots for systolic blood pressure. MD = 0.97, 95%CI: -1.20 to 3.04, P = 0.3580; I^2 =78%; E: Forest and funnel plots for diastolic blood pressure. MD = 2.75, 95%CI: 0.35-5.16, P = 0.0248; I^2 =89%; F: Forest and funnel plots for heart rate. MD = -1.35, 95%CI: -4.58 to 1.89, P = 0.4141; I^2 =90%.

A

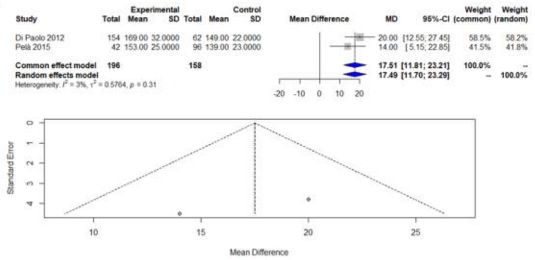

Funnel plot: some asymmetry; potential publication bias

B

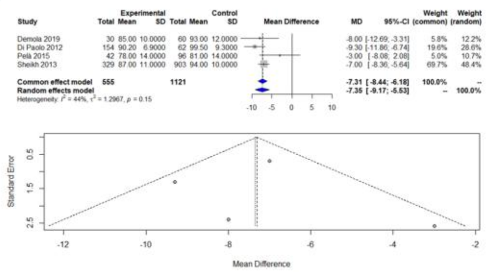

Funnel plot: some asymmetry; potential publication bias

C

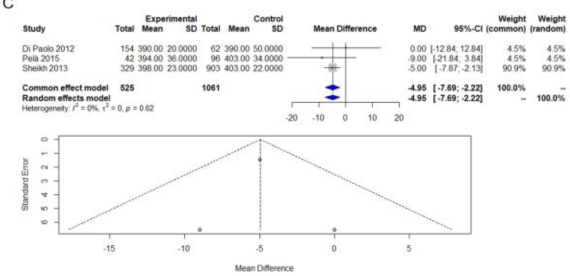

Funnel plot: some asymmetry; potential publication bias

D

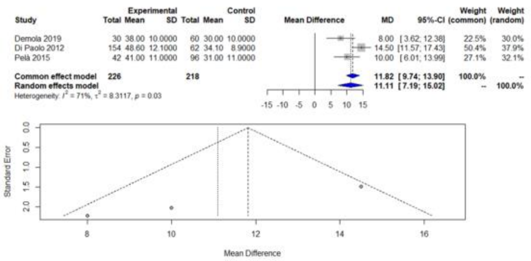

Funnel plot: some asymmetry; potential publication bias

E

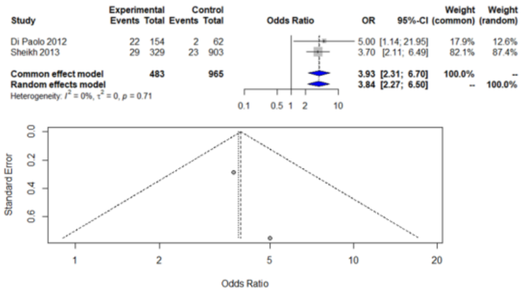

Funnel plot: some asymmetry; potential publication bias

F

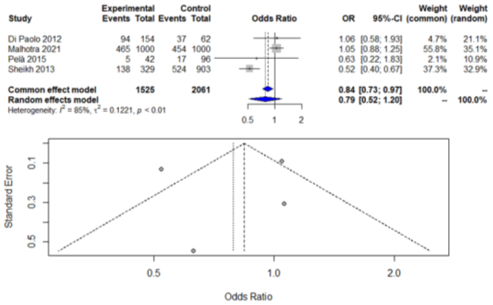

Funnel plot: some asymmetry; potential publication bias

G

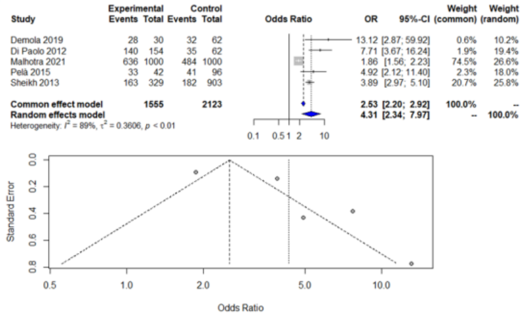

Funnel plot: asymmetry; publication bias

H

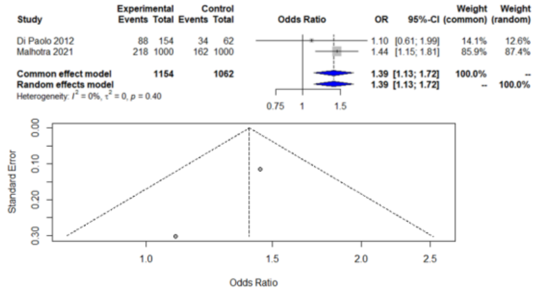

Funnel plot: some asymmetry; potential publication bias

I

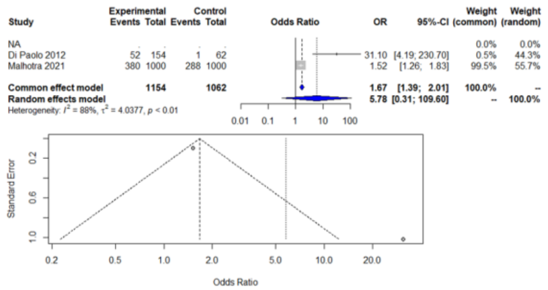

Funnel plot: asymmetry; publication bias

J

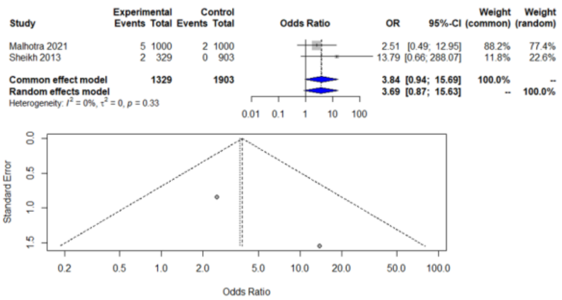

Funnel plot: some asymmetry; potential publication bias

K

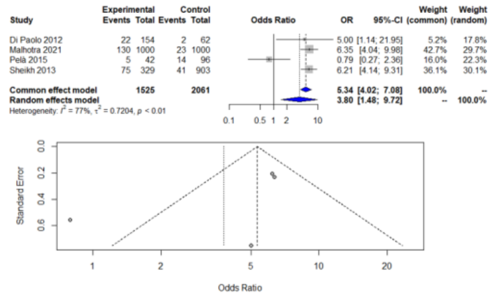

Funnel plot: asymmetry; publication bias

L

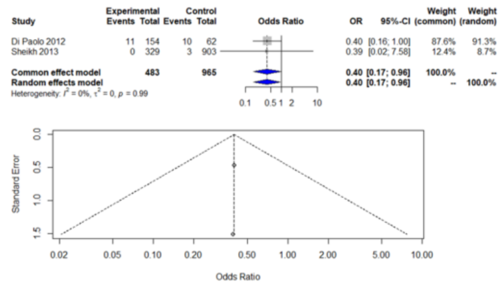

Funnel plot: some asymmetry; potential publication bias

M

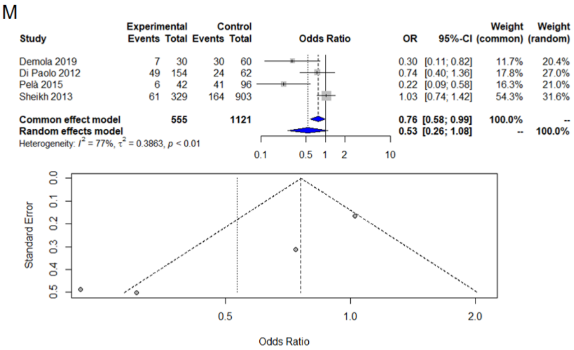

Funnel plot: asymmetry; publication bias

O

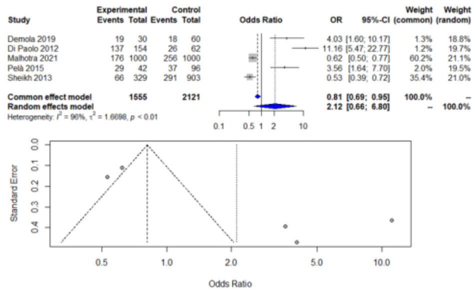

Funnel plot: asymmetry; publication bias

N

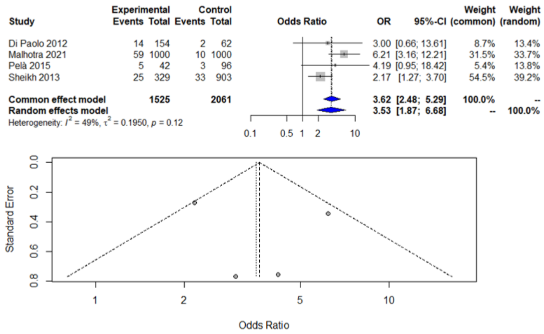

Funnel plot: symmetry; no publication bias

P

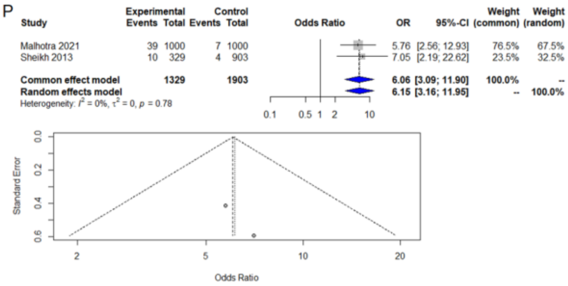

Funnel plot: some asymmetry; potential publication bias

Q

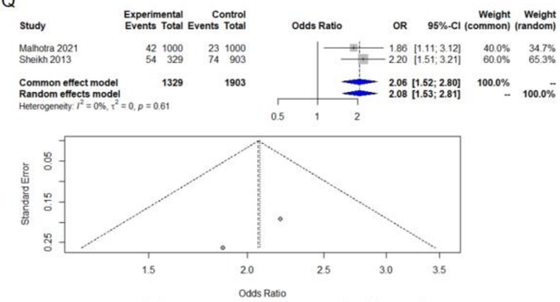

Funnel plot: some asymmetry; potential publication bias

Supplementary Figure 3 Electrocardiographic data. A: Forest and funnel plots for PR interval. Mean difference (MD) = 17.49, 95%CI: 11.70-23.29, P < 0.0001; I^2 = 3%; B: Forest and funnel plots for QRS complex. MD = -7.35, 95%CI: -9.17 to -5.53, P < 0.0001; I^2 = 44%; C: Forest and funnel plots for QTc interval. MD = -4.95, 95%CI: -7.69 to -2.22, P = 0.0004; I^2 = 0%; D: Forest and funnel plots for R1/S5 wave. MD = 11.11, 95%CI: 7.19-15.02, P < 0.0001; I^2 = 71%; E: Forest and funnel plots for atrioventricular block. Odds ratio (OR) = 3.84, 95%CI: 2.27-6.50, P < 0.0001; I^2 = 0%; F: Forest and funnel plots for sinus bradycardia. OR = 0.79, 95%CI: 0.52-1.20, P = 0.2692; I^2 = 85%; G: Forest and funnel plots for ST-segment elevation. OR = 4.31, 95%CI: 2.34-7.97, P < 0.0001; I^2 = 89%; H: Forest and funnel plots for ascending concave ST-segment elevation (domed). OR = 1.39, 95%CI: 1.13-1.72, P = 0.0020; I^2 = 0%; I: Forest and funnel plots for ascending convex ST-segment elevation. OR = 5.78, 95%CI: 0.31-109.60, P = 0.2424; I^2 = 88%; J:

Forest and funnel plots for ST-segment elevation. OR = 3.69, 95%CI: 0.87-15.63, P = 0.0767; I^2 = 0%; K: Forest and funnel plots for inverted T-wave. OR = 3.80, 95%CI: 1.48-9.72, P = 0.0054; I^2 = 77%; L: Forest and funnel plots for pathologic Q wave. OR = 0.40, 95%CI: 0.17-0.96, P = 0.0392; I^2 = 0%; M: Forest and funnel plots for right bundle branch block. OR = 0.53, 95%CI: 0.26-1.08, P = 0.0809; I^2 = 77%; N: Forest and funnel plots for left atrial enlargement. OR = 3.53, 95%CI: 1.87-6.68, P = 0.0001; I^2 = 49%; O: Forest and funnel plots for left ventricular hypertrophy. OR = 2.12, 95%CI: 0.66-6.80, P = 0.2088; I^2 = 96%; P: Forest and funnel plots for right atrial enlargement. OR = 6.15, 95%CI: 3.16-11.95, P < 0.0001; I^2 = 0%; Q: Forest and funnel plots for right ventricular hypertrophy. OR = 2.08, 95%CI: 1.53-2.81, P < 0.0001; I^2 = 0%.

A

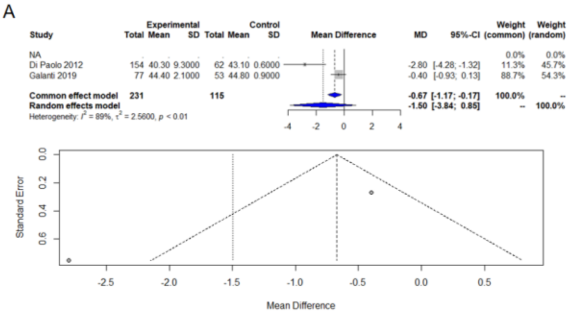

Funnel plot: asymmetry; publication bias

B

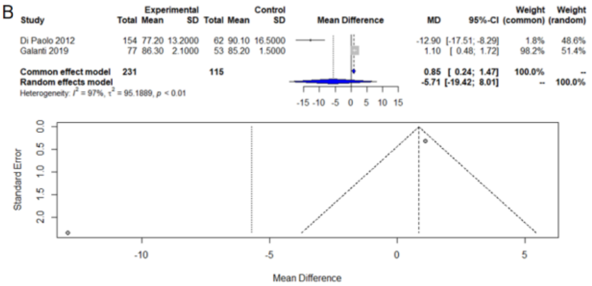

Funnel plot: some asymmetry; potential publication bias

C

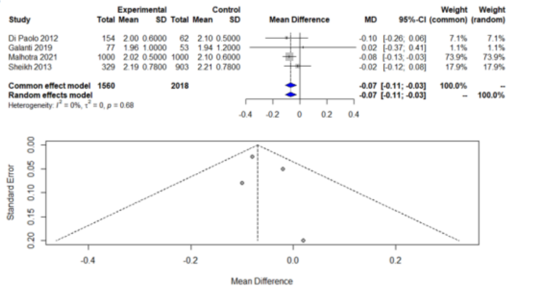

Funnel plot: some asymmetry; potential publication bias

D

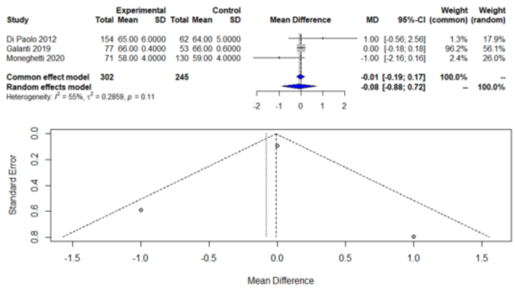

Funnel plot: some asymmetry; potential publication bias

E

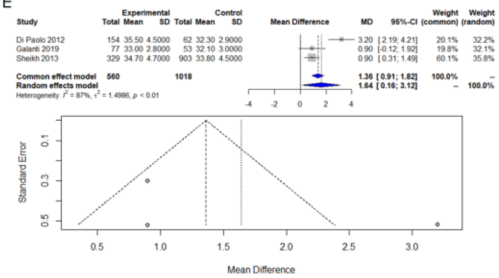

Funnel plot: asymmetry; publication bias

F

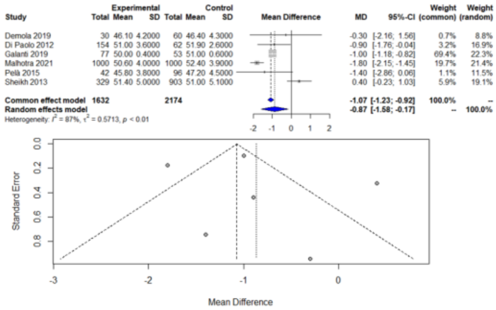

Funnel plot: some asymmetry; potential publication bias

G

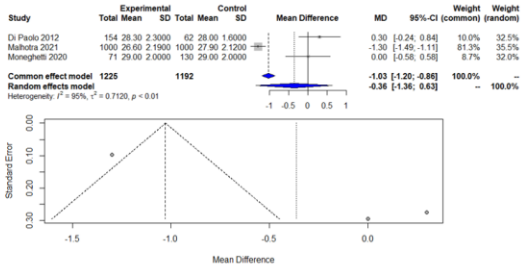

Funnel plot: asymmetry; publication bias

H

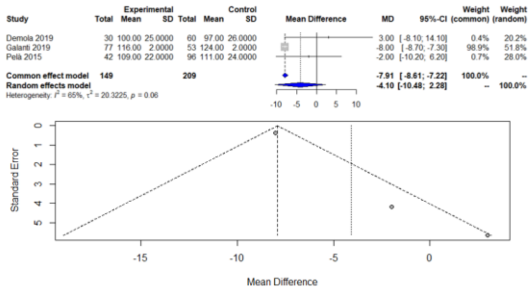

Funnel plot: asymmetry; publication bias

I

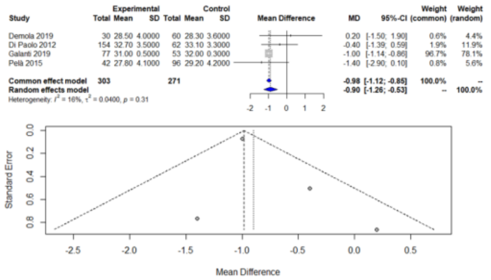

Funnel plot: some asymmetry; potential publication bias

J

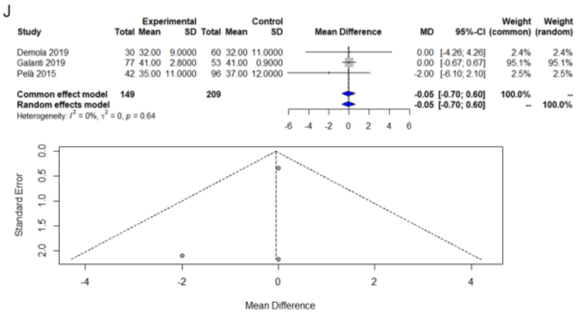

Funnel plot: asymmetry; publication bias

K

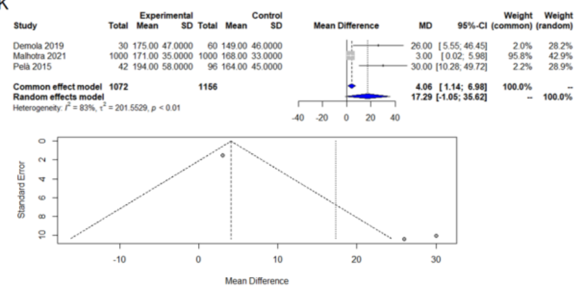

Funnel plot: asymmetry; publication bias

L

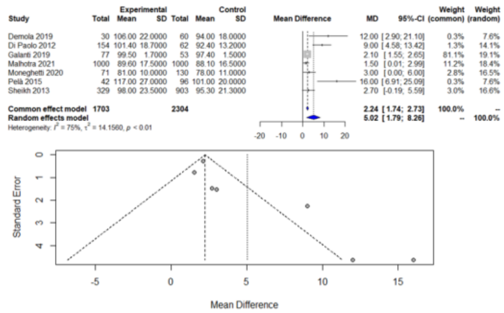

Funnel plot: asymmetry; publication bias

M

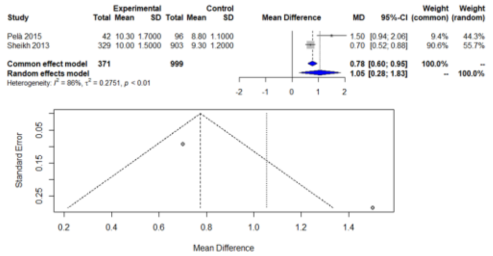

Funnel plot: asymmetry; publication bias

N

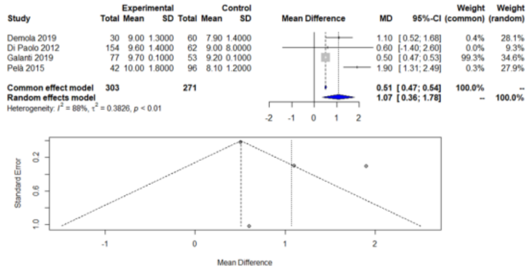

Funnel plot: asymmetry; publication bias

O

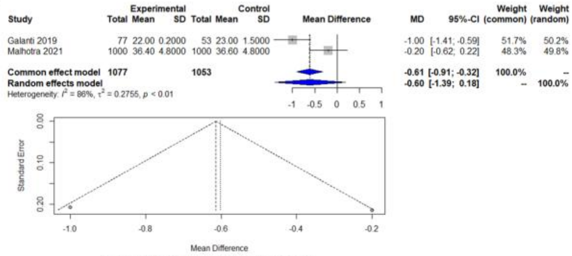

Funnel plot: symmetry; no publication bias

P

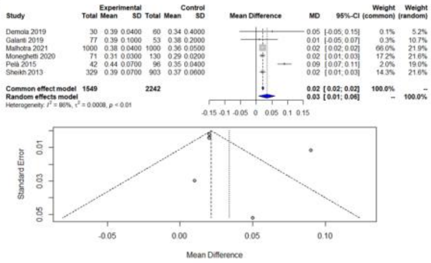

Funnel plot: asymmetry; publication bias

Q

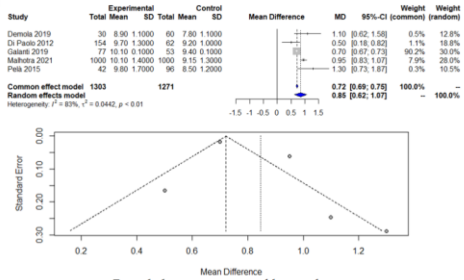

Funnel plot: asymmetry; publication bias

R

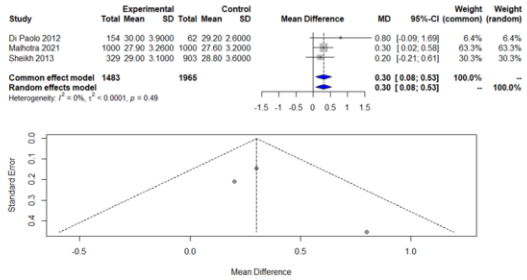

Funnel plot: asymmetry; publication bias

Supplementary Figure 4 Echocardiographic parameters. A: Forest and funnel plots for A wave. Mean difference (MD) = -1.50, 95%CI: -3.84 to 0.85, *P* = 0.2106; I^2 = 89%; B: Forest and funnel plots for E wave. MD = -5.71, 95%CI: -19.42 to 8.01, *P* = 0.4148; I^2 = 97%**;** C: Forest and funnel plots for E/A ratio. MD = -0.07, 95%CI: -0.11 to -0.03, *P* = 0.0011; I^2 = 0%; D: Forest and funnel plots for left ventricular ejection fraction. MD = -0.08, 95%CI: -0.88 to 0.72, *P* = 0.8412; I^2 = 55%; E: Forest and funnel plots for left atrial diameter. MD = 1.64, 95%CI: 0.16-3.12, *P* = 0.0296; I^2 = 87%; F: Forest and funnel plots for left ventricular end-diastolic diameter/dimension. MD = -0.87, 95%CI: -1.58 to -0.17, *P* = 0.0153; I^2 = 87%; G: Forest and funnel plots for left ventricular end-diastolic diameter/dimension indexed. MD = -0.36, 95%CI: -1.36 to 0.63, P = 0.4721; I^2 = 95%; H: Forest and funnel plots for left ventricular end-diastolic volume. MD = -4.10, 95%CI: 10.48; 2.28, P = 0.2080; I^2 = 65%; I: Forest and funnel plots for left ventricular end-systolic diameter/dimension. MD = -0.90, 95%CI: -1.26 to -0.53, P < 0.0001; I^2 = 16%; J: Forest and funnel plots for left ventricular end-systolic volume. MD = -0.05, 95%CI: -0.70 to 0.60, P = 0.8789; I^2 = 0%; K: Forest and funnel plots for left ventricular mass. MD = 17.29, 95%CI: -1.05 to 35.62, P = 0.0646; I^2 = 82.7%; L: Forest and funnel plots for left ventricular mass index. MD = 5.02, 95%CI: 1.79-8.26, P = 0.0023; I^2 = 75%; M: Forest and funnel plots for maximal wall thickness. MD = 1.05, 95%CI: 0.28-1.83, P = 0.0080 I^2 = 86%; N: Forest and funnel plots for posterior wall thickness. MD = 1.07, 95%CI: 0.36-1.78, P = 0.0033; I^2 = 88%; O: Forest and funnel plots for right ventricular diameter. MD = -0.60, 95%CI: -1.39 to 0.18, P = 0.1324; I^2 = 86%; P: Forest and funnel plots for relative wall thickness. MD = 0.03, 95%CI: 0.001-0.06, P = 0.0126; I^2 = 86%; Q: Forest and funnel plots for ventricular septum/septal wall thickness. MD = 0.85, 95%CI: 0.62-1.07, P < 0.0001; I^2 = 83%; R: Forest and funnel plots for aortic root. MD = 0.30, 95%CI: 0.08-0.53, P = 0.0087; I^2 = 0%.

Supplementary Table 1 Research strategy

Number	PubMed search–November 29, 2024	Records
1	(("Athletes"[Mesh]) AND "Cardiomegaly, Exercise-Induced"[Mesh]) AND "Adolescent"[Mesh]	31
2	(("Athletes"[Mesh]) AND "Adolescent"[Mesh]) AND "Adaptation, Physiological"[Mesh]	141
3	'Sport' AND ‘Athlete’ AND 'adolescent' AND 'myocardial adaptation'	79
4	'Sport' AND ‘Athlete’ AND 'adolescent' AND 'cardiac adaptation' with limits (clinical trials; adolescent: 13 – 18)	80
5	'Sport' AND ‘Athlete’ AND 'adolescent' AND 'cardiac remodeling'	146
6	'Sport' AND ‘Athlete’ AND 'adolescent' AND 'Electrocardiography' with limits (clinical trials)	24
7	'Sport' AND ‘Athlete’ AND 'adolescent' AND 'Echocardiography' with limits (clinical trials)	39

8	'Sport' AND 'Athlete' AND 'adolescent' AND 'Magnetic Resonance Imaging' with limits (clinical trials)	187
	Overall record	727
	No duplicates	620
	Manual search	0
	Excluded per title/Abstract	555
	Full text	65
	Included	7

Supplementary Table 2 Excluded studies

Studies	
Part A	Number of studies
Respiratory/metabolic/immune adaptation to exercise	7
Psychological adaptation	4
Physiological adaptation/response	54
Bone adaptation	13
Muscle adaptation	23
Temperature response	5
Testing performance	19
Training/physical fitness	20
Cardiac damage/markers	4
Injuries	43
Surgery	43
Genetics	2
Blood test	6
Hydration/nutrition	7
Cardiac remodeling	5
Cardiomyopathy/pathological hypertrophy	6
Impact of puberty/growth	3
Adults	87
Children < 11 years	3

Review article	32
Case report	5
Non-athletes	162
Study design	1
Animal	1
	555
Part B	Reason for exclusion
Kozupitsa GS, Babkin SM, Kel'tsev DI. Cardiac diastolic function in children and adolescents during prompt and long-term adaptation to physical exercise. *Kardiologiia* 1992; 32: 74-77	Not on racial disparities
Aymen Mohamed BA, Anis G, Ahmed FR, et al. Correlation between changes in electrocardiographic and echocardiographic measurements and the nature of the sport practiced. *Ann Cardiol Angeiol (Paris)*. 2023;72(2):101580	Not on racial disparities
Birat A, Ratel S, Dodu A, et al. A long-duration race induces a decrease of left ventricular strains, twisting mechanics and myocardial work in trained adolescents. *Eur J Sport Sci*. 2023;23(7):1394-1404	Not on racial disparities
Wernstedt P, Sjöstedt C, Ekman I, et al. Adaptation of cardiac morphology and function to endurance and strength training. A comparative study using MR imaging and echocardiography in males and females. *Scand J Med Sci Sports*. 2002;12(1):17-25	Not on racial disparities
Perkins DR, Talbot JS, Lord RN, et al. Adaptation of Left Ventricular Twist Mechanics in Exercise-Trained Children Is Only Evident after the Adolescent Growth Spurt. *J Am Soc Echocardiogr*. 2024;37(5):538-549	Not on racial disparities
Stavrou V, Tsarouhas K, Karetsi E, Michos P, Daniil Z, I Gourgoulianis K. Adolescent Finswimmers: Early Myocardial Adaptations in Different Swimming Styles. *Sports (Basel)*. 2018;6(3):78	Not on racial disparities/No relevant subgroup
Rodriguez-López AM, Javier G, Carmen P, et al. Athlete Heart in Children and Young Athletes. Echocardiographic Findings in 331 Cases. *Pediatr Cardiol*. 2022;43(2):407-412	Not on racial disparities/No relevant subgroup
Galetta F, Franzoni F, D'alessandro C, et al. Body composition and cardiac	Not on racial

dimensions in elite rhythmic gymnasts. *J Sports Med Phys Fitness*. 2015;55(9):946-952	disparities/No relevant subgroup
Zacher J, Blome I, Schenk A, Gorr E. Cardiac adaptations in elite female football- and volleyball-athletes do not impact left ventricular global strain values: a speckle tracking echocardiography study. *Int J Cardiovasc Imaging*. 2020;36(6):1085-1096	Not on racial disparities/No relevant subgroup
Rowland TW, Unnithan VB, MacFarlane NG, Gibson NG, Paton JY. Clinical manifestations of the 'athlete's heart' in prepubertal male runners. *Int J Sports Med*. 1994;15(8):515-519	Not on racial disparities/No relevant subgroup
Gerling S, Pollinger T, Dechant MJ, Melter M, Krutsch W, Michel H. Coronary artery z score values in adolescent elite male soccer players. *Cardiol Young*. 2021;31(3):381-385	Not on racial disparities/No relevant subgroup
Zdravkovic M, Milovanovic B, Hinic S, et al. Correlation between ECG changes and early left ventricular remodeling in preadolescent footballers. *Physiol Int*. 2017;104(1):42-51	Not on racial disparities/No relevant subgroup
Vasiliauskas D, Venckūnas T, Marcinkeviciene J, Bartkeviciene A. Development of structural cardiac adaptation in basketball players. *Eur J Cardiovasc Prev Rehabil*. 2006;13(6):985-989	Not on racial disparities/No relevant subgroup
Koch S, Cassel M, Linné K, Mayer F, Scharhag J. ECG and echocardiographic findings in 10-15-year-old elite athletes. *Eur J Prev Cardiol*. 2014;21(6):774-781	Not on racial disparities/No relevant subgroup
Petridis L, Kneffel Z, Kispéter Z, Horváth P, Sidó Z, Pavlik G. Echocardiographic characteristics in adolescent junior male athletes of different sport events. *Acta Physiol Hung*. 2004;91(2):99-109	Not on racial disparities/No relevant subgroup
Zdravkovic M, Perunicic J, Krotin M, et al. Echocardiographic study of early left ventricular remodeling in highly trained preadolescent footballers. *J Sci Med Sport*. 2010;13(6):602-606	Not on racial disparities/No relevant subgroup
Madeira RB, Trabulo M, Alves F, Pereira JG. Effects of chronic exercise training on left ventricular dimensions and function in young athletes. *Rev Port Cardiol*. 2008;27(7-8):909-922	Not on racial disparities/No relevant subgroup
Binnetoğlu FK, Babaoğlu K, Altun G, Kayabey Ö. Effects that different	Not on racial

types of sports have on the hearts of children and adolescents and the value of two-dimensional strain-strain-rate echocardiography. *Pediatr Cardiol*. 2014;35(1):126-139	disparities/No relevant subgroup
Thompson AJ, Cannon BC, Wackel PL, et al. Electrocardiographic abnormalities in elite high school athletes: comparison to adolescent hypertrophic cardiomyopathy. *Br J Sports Med*. 2016;50(2):105-110	Not on racial disparities/No relevant subgroup
Dawkins TG, Shave RE, Baggish AL, et al. Electrocardiographic changes following six months of long-distance triathlon training in previously recreationally active individuals. *Eur J Sport Sci*. 2020;20(4):553-562	Not on racial disparities/No relevant subgroup
Kösemen DS, Çetin S, Demirci D, Babaoğlu K. Evaluation of the Left Ventricular Myocardium Using Layer-Specific Strain Analysis in Adolescent Athletes Performing High-Intensity Interval Training. *Pediatr Cardiol*. 2024;45(4):770-779	Not on racial disparities/No relevant subgroup
Weiner RB, DeLuca JR, Wang F, et al. Exercise-Induced Left Ventricular Remodeling Among Competitive Athletes: A Phasic Phenomenon. *Circ Cardiovasc Imaging*. 2015;8(12):e003651	Not on racial disparities/No relevant subgroup
Pelliccia A, Avelar E, De Castro S, Pandian N. Global left ventricular shape is not altered as a consequence of physiologic remodeling in highly trained athletes. *Am J Cardiol*. 2000;86(6):700-A9	Not on racial disparities/No relevant subgroup
Suzic Lazic J, Dekleva M, Soldatovic I, et al. Heart rate recovery in elite athletes: the impact of age and exercise capacity. *Clin Physiol Funct Imaging*. 2017;37(2):117-123	Not on racial disparities/No relevant subgroup
Agrebi B, Tkatchuk V, Hlila N, Mouelhi E, Belhani A. Impact of specific training and competition on myocardial structure and function in different age ranges of male handball players. *PLoS One*. 2015;10(12):e0143609	Not on racial disparities/No relevant subgroup
Smith D, Deblois J, Wharton M, Rowland T. Influence of sex on ventricular remodeling in collegiate athletes. *J Sports Med Phys Fitness*. 2012;52(4):424-431	Not on racial disparities/No relevant subgroup
Szabo D, Nagy D, Melczer C, et al. Influencing Factors of Cardiac Adaptation in Adolescent Athletes. *Int J Sports Med*. 2021;42(13):1209-1221	Not on racial disparities/No relevant subgroup

Hoogsteen J, Hoogeveen A, Schaffers H, Wijn PF, van der Wall EE. Left atrial and ventricular dimensions in highly trained cyclists. *Int J Cardiovasc Imaging*. 2003;19(3):211-217	Not on racial disparities/No relevant subgroup
D'Ascenzi F, Cameli M, Lisi M, et al. Left atrial remodelling in competitive adolescent soccer players. *Int J Sports Med*. 2012;33(10):795-801	Not on racial disparities/No relevant subgroup
Miragoli M, Goldoni M, Demola P, et al. Left ventricular geometry correlates with early repolarization pattern in adolescent athletes. *Scand J Med Sci Sports*. 2019;29(11):1727-1735	Not on racial disparities/No relevant subgroup
Smith SA, Humphrey RH, Wohlford JC, Flint DL. Myocardial adaptation and weight fluctuation in college wrestlers. *Int J Sports Med*. 1994;15(2):70-73	Not on racial disparities/No relevant subgroup
Dores H, Mendes L, Dinis P, Cardim N, Monge JC, Santos JF. Myocardial deformation and volume of exercise: a new overlap between pathology and athlete's heart?. *Int J Cardiovasc Imaging*. 2018;34(12):1869-1875	Not on racial disparities/No relevant subgroup
Rowland T, Unnithan V, Roche D, Garrard M, Holloway K, Marwood S. Myocardial function and aerobic fitness in adolescent females. *Eur J Appl Physiol*. 2011;111(9):1991-1997	Not on racial disparities/No relevant subgroup
D'Ascenzi F, Solari M, Biagi M, et al. P-wave morphology is unaffected by training-induced biatrial dilatation: a prospective, longitudinal study in healthy athletes. *Int J Cardiovasc Imaging*. 2016;32(3):407-415	Not on racial disparities/No relevant subgroup
Kinoshita N, Onishi S, Yamazaki H, Katsukawa F, Yamada K. Recognition of left ventricular hypertrophy in new recruits of professional sumo wrestling. *J Sci Med Sport*. 2003;6(4):379-386	Not on racial disparities/No relevant subgroup
Yıldırım Ş, Binnetoğlu FK, Battal F, et al. Relation between QT Variables and Left Ventricular Geometry in Athletes and Obese Children. *Acta Med Port*. 2016;29(2):95-100	Not on racial disparities/No relevant subgroup
Krenc Z. Relationship Between Adaptive Morphological and Electrophysiological Remodeling of the Left Ventricle in Young Athletes After an 8-Month Period of Sports Training. *Pediatr Exerc Sci*. 2016;28(1):71-76	Not on racial disparities/No relevant subgroup

Pelà G, Crocamo A, Li Calzi M, et al. Sex-related differences in left ventricular structure in early adolescent non-professional athletes. *Eur J Prev Cardiol*. 2016;23(7):777-784	Not on racial disparities/No relevant subgroup
Kim JH, Noseworthy PA, McCarty D, et al. Significance of electrocardiographic right bundle branch block in trained athletes. *Am J Cardiol*. 2011;107(7):1083-1089	Not on racial disparities/No relevant subgroup
Simsek Z, Hakan Tas M, Degirmenci H, et al. Speckle tracking echocardiographic analysis of left ventricular systolic and diastolic functions of young elite athletes with eccentric and concentric type of cardiac remodeling. *Echocardiography*. 2013;30(10):1202-1208	Not on racial disparities/No relevant subgroup
Hanne-Paparo N, Wendkos MH, Brunner D. T wave abnormalities in the electrocardiograms of top-ranking athletes without demonstrable organic heart disease. *Am Heart J*. 1971;81(6):743-747	Not on racial disparities/No relevant subgroup 7 cases
Bjerring AW, Landgraff HE, Stokke TM, et al. The developing athlete's heart: a cohort study in young athletes transitioning through adolescence. *Eur J Prev Cardiol*. 2019;26(18):2001-2008	Not on racial disparities/No relevant subgroup
Csecs I, Czimbalmos C, Toth A, et al. The impact of sex, age and training on biventricular cardiac adaptation in healthy adult and adolescent athletes: Cardiac magnetic resonance imaging study. *Eur J Prev Cardiol*. 2020;27(5):540-549	Not on racial disparities/No relevant subgroup
Perkins DR, Talbot JS, Lord RN, et al. The influence of maturation on exercise-induced cardiac remodelling and haematological adaptation. *J Physiol*. 2022;600(3):583-601	Not on racial disparities/No relevant subgroup
Hauser M, Petzuch K, Kühn A, et al. The Munich Triathlon Heart Study: ventricular function, myocardial velocities, and two-dimensional strain in healthy children before and after endurance stress. *Pediatr Cardiol*. 2013;34(3):576-582	Not on racial disparities/No relevant subgroup
Lazic JS, Tadic M, Antic M, et al. The relationship between right heart and aerobic capacity in large cohort of young elite athletes. *Int J Cardiovasc Imaging*. 2019;35(6):1027-1036	Not on racial disparities/No relevant subgroup

Whyte GP, George K, Sharma S, et al. The upper limit of physiological cardiac hypertrophy in elite male and female athletes: the British experience. *Eur J Appl Physiol*. 2004;92(4-5):592-597	Not on racial disparities/No relevant subgroup
D'Ascenzi F, Solari M, Mazzolai M, et al. Two-dimensional and three-dimensional left ventricular deformation analysis: a study in competitive athletes. *Int J Cardiovasc Imaging*. 2016;32(12):1697-1705	Not on racial disparities/No relevant subgroup
Valente-Dos-Santos J, Coelho-e-Silva MJ, Vaz V, et al. Ventricular mass in relation to body size, composition, and skeletal age in adolescent athletes. *Clin J Sport Med*. 2013;23(4):293-299	Not on racial disparities/No relevant subgroup
Sagiv M, Sagiv M, Ben-Sira D. Weight lifting training and left ventricular function in adolescent subjects. *J Sports Med Phys Fitness*. 2007;47(3):329-334	Not on racial disparities/No relevant subgroup
Forså MI, Bjerring AW, Haugaa KH, et al. Young athlete's growing heart: sex differences in cardiac adaptation to exercise training during adolescence. *Open Heart*. 2023;10(1):e002155	Not on racial disparities/No relevant subgroup
Riding NR, Salah O, Sharma S, et al. ECG and morphologic adaptations in Arabic athletes: are the European Society of Cardiology's recommendations for the interpretation of the 12-lead ECG appropriate for this ethnicity?. *Br J Sports Med*. 2014;48(15):1138-1143. doi:10.1136/bjsports-2012-091871	Adults/ 9 cases
Churchill TW, Petek BJ, Wasfy MM, et al. Cardiac Structure and Function in Elite Female and Male Soccer Players. *JAMA Cardiol*. 2021;6(3):316-325	Adults
Tomoto T, Sugawara J, Hirasawa A, Imai T, Maeda S, Ogoh S. Impact of short-term training camp on arterial stiffness in endurance runners. *J Physiol Sci*. 2015;65(5):445-449	Adults
Krustrup P, Hansen PR, Nielsen CM, et al. Structural and functional cardiac adaptations to a 10-week school-based football intervention for 9-10-year-old children. *Scand J Med Sci Sports*. 2014;24 Suppl 1:4-9	Children < 11 years
Beaumont A, Oxborough D, George K, et al. Superior cardiac mechanics without structural adaptations in pre-adolescent soccer players. *Eur J Prev Cardiol*. 2020;27(14):1494-1501	Children < 11 years

Griffet V, Guérard S, Galoisy-Guibal L, Caignault JR, Bernard F, Brion R. Normal values of the peak early diastolic Ea using myocardial tissue Doppler in 100 elite athletes]. *Arch Mal Coeur Vaiss*. 2007;100(10):809-815	Comparison between LVH and HCM
Sharma C, Dorobantu DM, Ryding D, et al. Investigating the Accuracy of Quantitative Echocardiographic-Modified Task Force Criteria for Arrhythmogenic Ventricular Cardiomyopathy in Adolescent Male Elite Athletes. *Pediatr Cardiol*. 2022;43(2):457-464.	Non-health athletes

Supplementary Table 3 Study objective and eligibility criteria

Ref.	Objective(s)	Eligibility criteria
Demola *et al*[38], 2019	To define physiological LV adaptation to exercise in African athletes and the mechanisms through which LV hypertrophy develops, to differentiate it from its pathological analogue. To assess a possible relationship between peculiar LV remodeling (more concentric hypertrophy) and hemodynamic response to physical exercise (*e.g.* greater BP response) in adolescent athletes of African ethnicity compared to Caucasians	-
Di Paolo *et al*[39], 2012	-	Each subject was judged to be free of patent cardiovascular disease on the basis of the history, physical examination (with BP < 140/90 mm Hg), and ECHO results
Galanti *et al*[40], 2019	To study cardiovascular and, specifically, LV remodeling in young African Americans compared to young Caucasian soccer players	Athletes with a previous personal or family history of cardiac or pulmonary disease, family history of premature (≤40 yr) sudden cardiac death or cardiomyopathy were excluded from the study
Malhotra *et al*[41], 2021	To examine electric and structural adaptations in heart of healthy mixed-race male soccer players and compare them with those of White and Black male soccer players. A mixed-race athlete was classified as an individual with 1 White parent of European origin and 1 Black parent of	Athletes with overt cardiomyopathy were excluded based on a normal exercise stress test/ECHO, 24-hour ECG monitor, and absence of scar on cardiovascular MRI before inclusion in the study

	African/Afro-Caribbean origin	
Moneghetti *et al*[42], 2020	To explore hypothesis that race, player position, and body composition would contribute to LV remodeling. To provide insights into race-specific and position differences in LV and function during pre-participation screening of collegiate ASF players	Participants with evidence of cardiomyopathy, significant valvular abnormalities, congenital heart disease, or inadequate endocardial definition during echocardiographic examination were excluded
Pelà *et al*[43], 2015	To determine whether LV responses to sport training are ethnicity-associated in the early adolescent age, when pubertal development may not be yet complete. To determine whether higher LVWT and LVM with preferential concentric remodeling in black adolescent athletes vs white counterparts are detectable at an amateur-level training as are in the elite-level sport context	Participants free from heart disease and, based on the questionnaires, engaged in organized football training for approximately 2.5 h twice/week
Sheikh *et al*[44], 2013	To identify the spectrum of physiological adaptation in highly trained adolescent BA	Selection criteria for controls were black ethnicity, age 14–18 years, sedentary lifestyle (≤2h of organized physical activity/week), absence of symptoms, drug history, family history of cardiomyopathy or premature (≤40 years) SCD, normal blood pressure and a structurally normal heart

Supplementary Table 4 **General characteristics of included cohort studies**

Ref.	Country site(s)	Sample size	Black athletes, *n* (%)	White athletes	Sport/training intensity and other comments

Demola *et al*[38], 2019	Italy (Parma)	90	30/90 (33.3%). Origin: Central/West Africa, namely Burkina Faso, Cameroon, Ghana, Ivory Coast, Nigeria, and Senegal	60/90 (66.7%)	Athletics (amateur-level) in different endurance disciplines, ~7 hours/week
Di Paolo *et al*[39], 2012	Italy (Rome)	216	154/216 (71.3%). Origin: 8 countries (Algeria, Burkina Faso, Cameroon, Gambia, Guinea, Malawi, Nigeria, and Zimbabwe)	62/216 (28.7%). Caucasian athletes of Italian descent	Soccer players. 6-day training session/week, each ≥ 2 h, including either general conditioning or specific technical programs. Black athletes trained and competed for ≥ 3 consecutive years and represented best competitors in the < 17-year-old category
Galanti *et al*[40], 2019	Italy (Florence)	130	77/130 (59.2%). Afro–Caribbean/African-Americans	53/130 (40.8%) – matched	Soccer players. Athletes were members of the same soccer team with similar lifestyle. 6 times/week, each training session lasting ≥ 2 h
Malhotra *et al*[41], 2021	United Kingdom 2015 to 2018	3000 (3 subgroups)	1000/3000 (33.3%). African (61%) or Caribbean (39%) origin	1000/3000 (33.3%)	Elite soccer players. 1000/3000 (33.3%) were mixed-race
Moneghetti *et al*[42], 2020	United States 2008 to 2016	230	71/230 (30.9%). African American	130/230 (56.5%). Caucasian	American style football. Remaining 12 % of players were of Asian (n = 5), Hispanic (n = 2), Hawaiian (n = 2), or other/unknown (n = 19) race
Pelà *et al*[43],	Italy	138	42/138 (30.4%). Origin: West-	96/138 (69.6%).	Football (in local, amateur-level leagues).

2015	(Parma) 20062013		Africa (i.e., Bantu, because their families immigrated to Italy from Burkina Faso, Cameroon, Ghana, Ivory Coast, Nigeria, or Senegal and were permanently established in Parma city or its area). 24 were born in Italy, whereas the remaining 18, born in Africa, have been living in Italy for at least 6 years	Italian descent; born in the Parma area or had been living there for at least 6 years	Approximately 2.5 hours twice/week. Subjects participated (usually during weekends) in one amateur-level local competition; the total sport load was ~8 hours/week in both groups. Athletes were junior or senior high school
Sheikh *et al*[44], 2013	United Kingdon and France 1996 to 2011	1232	329/1232 (26.7%). African/Afro-Caribbean	903/1232 (73.3%)	Athletes competed in a wide range (n=29) of sporting disciplines. Competing at the regional, national, or international level

Supplementary Table 5 Electrocardiographic and echocardiographic study details

Ref.	Electrocardiography (ECG)	Echocardiography (ECHO)
Demola *et al*[38], 2019	All participants underwent physical examinations with 12 lead resting ECG. S1/R5 in precordial leads	All participants underwent physical examinations with ECHO and ergometer stress test. M-mode, two-dimensional, and Doppler

	were calculated using the Sokolow-Lyon voltage criteria to assess the presence of ECG-based LV hypertrophy. Analysis of ECG also includes the innovative parameter introduced for the stratification of arrhythmic risk, e.g. QT dispersion (maximum QT interval minus minimum QT interval, QTd). The latter is an index of the spatial dispersion of ventricular recovery times and, therefore, is an index of in homogeneity potentially involved in the genesis of arrhythmias.	ECHO were performed by an ultrasonography-experienced cardiologist, using a commercially available, multi-hertz sector, 2–4 MHz probe-equipped machine (Vivid S5, GE Healthcare, USA). The interventricular septal (SWT) and posterior wall (PWT) thicknesses, systolic (ESD) and diastolic (EDD) LV diameters, absolute left ventricular mass (LVM) and indexed to body surface area (LVM/BSA) were calculated. LVM was also normalized to height 2.7, an estimate of lean body mass. RWT was calculated as: (SWT + PWT)/EDD. According to the ASE guidelines, we calculate LV remodeling categories (normal, concentric remodeling, concentric and eccentric hypertrophy) in the two groups, based on LVM and RWT. Simpson's biplane rule-based end-diastolic (EDV) and systolic (ESV) volumes and ejection fraction (EF) were calculated, while Fractional Shortening (FS) was: [(EDV − ESV)/EDV] × 100. Mitral inflow pattern was analyzed from apical 4-chamber view and E and A waves and their ratio were considered as peak flow velocity and time velocity integral, in order to evaluate the conventional diastolic function
Di Paolo *et al*[39], 2012	Standard 12-lead ECGs were per formed with the subject in the supine position after a few minutes of	Two-dimensional and Doppler ECHO studies were performed with commercially available instruments (Esaote Italia, Genoa,

	rest during quiet respiration and recorded at 25 mm/s. We measured heart rate (beats/min), PR interval (ms), QRS duration (ms), QT interval corrected for the heart rate (s), presence of Q waves (≥ 2 mm in depth in ≥2 leads), R/S-wave amplitude in precordial leads (S1 R5) (mm), and Sokolow-Lyon criterion for LV hypertrophy (positive if ≥ 35 mm), presence and shape (concave or domed) of ST-segment elevation (≥ 1 mm, in ≥ 2 contiguous leads), presence of J-wave (≥ 1 mm), or ST-segment slurring (18), T-wave inversion (≥ 2 mm in depth in ≥ 2 contiguous leads, with exclusion of III and aVR), and flat/biphasic T-wave pattern (in ≥ 2 contiguous leads)	Italy, and Philips Medical Systems, Bothell, Washington). Images of heart were obtained in multiple cross-sectional planes by using standard transducer positions. M-mode echo cardiograms were derived from 2-dimensional images under direct anatomic visualization and recorded at 100 mm/s. Measurements of end-diastolic and end-systolic LV cavity dimensions, anterior ventricular septal, and posterior free wall thicknesses were obtained as previously recommended. LV mass was calculated by using the formula of Devereux and was indexed to body surface area (BSA). Relative wall thickness (h/r) was the ratio of septal and posterior free wall thicknesses to LV ventricular cavity diameter. Ejection fraction was assessed from end-diastolic and end-systolic LV volumes, in the apical 4-chamber view, and quantified according to the modified Simpson rule. Parameters of LV filling was obtained with pulsed Doppler ECHO.
Galanti *et al*[40], 2019	Standard 12-lead ECG was performed with the subject supine, after a few minutes of rest with normal breathing, and recorded at 25mm/s. We measured heart rate (beats/min), PR interval (ms), QRS duration (ms), QT interval corrected for the heart rate (s) [13],	ECHO was conducted by 2 experienced and certified cardiologists using a commercially available ultrasound system: iE33 Philips Medical System (Bothell, WA). These specialists work together and therefore the reproducibility of data is high and the inter-observer variability low (< 5%). Furthermore, at least 5 double blind echo

	presence of Q waves (≥2 mm in depth in ≥2 leads), R/S-wave amplitude in precordial leads (S1 + R5) (mm), and Sokolow-Lyon criterion for LV hypertrophy (positive if ≥35mm) , presence and shape (concave or domed) of ST-segment elevation (≥1 mm, in ≥2 contiguous leads), presence of J wave (≥1mm), or ST-segment slurring, T-wave inversion (≥2 mm in depth in ≥2 contiguous leads, with exclusion of III and a VR), and flat/biphasic T-wave pattern (in ≥2 contiguous leads)	tests were carried out after 3 days, in order to confirm the overlap of the data obtained
Malhotra *et al*[41], 2021	12-lead ECG was interpreted in accordance with international recommendations	ECHO was performed in accordance with standard American and European protocols
Moneghetti *et al*[42], 2020	-	Athletic screening protocol included: (a) 2-D and color Doppler left parasternal long- and short-axis views at the aortic valve level to assess coronary ostia and at the papillary muscle level to assess LV mass and volume; and (b) 2-D and color Doppler apical 4-chamber view to allow quantitative assessment of LV systolic and diastolic function (E, lateral E′) as well as left atrial size. Athletes with findings outside the normal range as defined by the American Society of Echocardiography or sub-optimal images were referred

		for a complete echocardiographic study
Pelà *et al*[43], 2015	12-lead, 25 mm/s, supine position ECGs were interpreted (Corrado et al., 2010) by three investigators (G. P., M. L. C.,A. C.) blinded to the type of subject. Heart rate (HR), QRS axis, PR interval, QRS duration, and corrected QT interval were measured. S1/R5 in precordial leads were calculated using the Sokolow Lyon voltage criteria (positive if ≥ 35 mm) to define the presence of LVH. Prevalence of Q waves (≥ 2 mm in depth in two or more adjacent leads), presence and shape (concave or domed) of ST-segment elevation (≥ 1 mm in two or more adjacent leads), and prevalence of inverted T waves (≥ 2 mm in depth in two or more adjacent leads, excluding aVR and III) were also assessed.	M-mode, 2-D, and Doppler ECHO were performed by one ultrasonography-experienced cardiologist using a commercially available, multi-hertz sector, 2–4 MHz probe equipped machine (Aspen, Siemens Acuson, Mountain View, California, USA). With the subject on the left lateral position, images based on 3 consecutive heart cycles were obtained from standard projections. The highest value of diastolic thickness between septum and posterior LV wall– both measured at the parasternal long-axis view according to Penn convention was considered as the maximal wall thickness (MWT), with end-systolic and diastolic LV diameters measured in the same projection. RWT was calculated as (thickness of septum + thickness of posterior wall)/LV end diastolic diameter (LVEDD), using the 0.42 cutoff to define eccentric (≤ 0.42) or concentric (≥ 0.42) remodeling. Penn convention-based LVM also was indexed, when necessary, to body surface area (BSA). Simpson's biplane rule-based end-diastolic and systolic LV volumes and ejection fraction were calculated, whereas fractional shortening was [(LVEDD– LV end-systolic diameter)/LVEDD] × 100. Blood flow across the mitral valve was

		monitored using the pulsed-Doppler technique in the apical four chamber view, with the sample volume placed at the tip of the valve. The blood flow profile contains diastolic E and A waves, and peak flow velocity and its time integral were measured for each wave. The intra-observer percentage variability for MWT was < 3.5
Sheikh *et al*[44], 2013	Standard 12-lead ECGs were performed. Relating to repolarization abnormalities, ST-segment shift was considered significant if ≥0.1 mV in ≥2 contiguous leads. Early repolarization pattern was defined as J-point elevation ≥0.1 mV in ≥2 contiguous non-anterior leads. T-wave inversion was considered significant if ≥−0.1 mV in ≥2 leads (excluding aVR, V1 and III in isolation). Biphasic T-wave inversion was considered abnormal if the negative deflection of the T-wave exceeded ≥−0.1 mV. The distribution of T-wave inversions was categorized into anterior (V1–V4), inferior (II, III, aVF) and lateral (I, aVL, V5, V6). Deep T-wave inversions were defined as a T-wave deflection ≥−0.2 mV. All ECGs were read independently by two authors in the UK and France.	2-D ECHO was performed using either a GE Vivid I (Tirat), Philips Sonos 7500, iE33 or CPX50 (Bothel). Standard views were obtained and cavity and wall thickness measurements performed using established guidelines. Left atrial (LA) diameter and left ventricular (LV) internal diameter were measured from the parasternal long axis view. Left ventricular wall thickness was measured in the parasternal short-axis view, at the levels of the mitral valve and papillary muscles; the greatest measurement was defined as the maximum left ventricular wall thickness (mLVWT). LVH was defined as an mLVWT >12mm. Left ventricular mass was calculated with the formula of Devereux. Relative LV wall thickness (RLVWT) was calculated by dividing the sum of the LV septal and posterior wall thicknesses in diastole by the end diastolic LV internal diameter. 2-D continuous-Doppler and pulsed-Doppler imaging were performed using standard

parasternal and apical views. A cardiologist blinded to the athlete's identity reviewed all scans

Supplementary Table 6 Patient baseline characteristics (Black vs White), *n* (%)

Ref.	Age (year), mean ± SD	Male	Height (cm)	Weight (kg)	BMI (kg/m²)	BSA (m²)	Training (hours/week)	SBP (mmHg)	DBP (mmHg)	HR (bpm)
Demola *et al*[38], 2019	13.8±1.6 (n=30) Vs 13.3±1.5 (n=60)	30/30 (100%) Vs 60/60 (100%)	168.0±8.0 (n=30) Vs 164.0±12.0 (n=60)	56.8±10.9 (n=30) Vs 53.1±13.5 (n=60)	19.9±2.3 (n=30) Vs 19.4±3.0 (n=60)	1.64±0.19 (n=30) Vs 1.56±0.25 (n=60)	7.0±1.8 (n=30) Vs 6.3±2.0 (n=60)	113±13 (n=30) Vs 105±12 (n=60), p=0.018	71±8 (n=30) Vs 64±9 (n=60), p=0.006	70±8 (n=30) Vs 76±11 (n=60), p=0.005
Di Paolo *et al*[39], 2012	15.9±0.7 Vs 16.5±1.1 years, p<0.01	154/154 (100%) Vs 62/62 (100%)	-	-	-	1.80±0.12 (n=154) Vs 1.85±0.11 (n=62), p=0.009	-	-	-	58.0±9.0 (n=154) Vs 58.0±9.0 (n=62)
Galanti *et al*[40], 2019	17.0±0.5 (n=77) Vs 18.0±0.8	-	173.0±1.1 (n=77) Vs 174.0±0.9	65.0±1.3 (n=77) Vs	21.4±0.2 (n=77) Vs	-	-	115±0.6 (n=77) Vs 116±1.3	73.0±0.5 (n=77) Vs 70.0±1.5	66.8±0.8 (n=77) Vs 64.1±2.0

	(n=53)		(n=53)	66.0±1.0 (n=53)	21.8±0.2 (n=53)			(n=53)	(n=53), p=0.04	(n=53)
Malhotra *et al*[41], 2021	All: 16.4±1.3 (n=3000)	All: 3000/3000 (100%)	-	-	-	-	-	-	-	-
Moneghetti *et al*[42], 2020	18.2±1.0 (n=71) Vs 18.6±1.3 (n=130), p=0.011	71/71 (100%) Vs 130/130 (100%)	185.0±6.0 (n=71) Vs 190.0±6.0 (n=130), p<0.001	98.0±19.0 (n=71) Vs 106±18.0 (n=130), p=0.002	28.5±4.2 (n=71) Vs 29.4±4.0 (n=130), p	2.23±0.24 (n=71) Vs 2.36±0.22 (n=130), p<0.001	-	129±13.0 (n=71) Vs 129±11.0 (n=130)	74.0±8.0 (n=71) Vs 70.0±9.0 (n=130), p=0.014	62.0±10.0 (n=71) Vs 62.0±9.0 (n=130)
Pelà *et al*[43], 2015	14.3±1.8 (n=42) Vs 13.9±1.6 (n=96)	42/42 (100%) Vs 96/96 (100%)	168.0±8.0 (n=42) Vs 167.0±12.0 (n=96)	57.0±10.0 (n=42) Vs 56.0±13.0 (n=96)	20.2±2.5 (n=42) Vs 19.9±2.9 (n=96)	1.64±0.17 (n=42) Vs 1.61±0.24 (n=96)	No difference	119.0±9.0 (n=42) Vs 118.0±10.0 (n=96)	72.0±8.0 (n=42) Vs 70.0±7.0 (n=96)	67.0±9.0 (n=42) Vs 72.0±10.0 (n=96)
Sheikh *et al*[44], 2013	16.4±1.3 (n=329) Vs 16.4±1.3 (n=903)	245/329 (74.5%) Vs 735/903 (81.4%),	-	-	-	1.90±0.21 (n=329) Vs 1.85±0.21	13.2±5.4 (n=329) Vs 11.6±4.1 (n=903),	113.6±13.4 (n=329) Vs 112.3±11.4 (n=903),	67.5±11.2 (n=329) Vs 68.4±9.2 (n=903)	-

	p<0.001	(n=903), p<0.001	p<0.001	p<0.001

Supplementary Table 7 Electrocardiographic measurements (Black vs White), ***n*** **(%)**

Ref.	**PR interval (ms)**	**QRS complex duration (ms)**	**QTc interval (ms)**	**QT dispersion**	**QRS axis (°)**	**R/S-wave voltages (S1 R5) (mm)**	**LV hypertrophy (Sokolow-Lyon criteria)**	**LA enlargement**	**RV hypertrophy**	**RA enlargement**	**STE (≥ 1mm in ≥ 2 leads)**	**ST-segment depression**	**J waves and/or slurring on STE**	**Pathological Q waves (≥ 2 mm in ≥ 2 leads)**	**ITW (≥ 2mm in ≥ 2 leads)**	**Flat/biphasic T waves (in ≥ 2 leads)**	**Sinus bradycardia (HR < 60 bpm)**	**Sinus arrhythmia**	**First-degree AV block (PR interval > 0.20 s)**	**Incomplete/ partial RBBB (QRS > 0.10 < 0.12 s)**
Demola *et al*[38], 2019	-	85.0±10.0 (n=30) Vs 93.0±12.0 (n=60), p=0.004	-	37.0±13.0 (n=30) Vs 27.0±8.0 (n=60), p<0.001	-	38.0±10.0 (n=30) Vs 30.0±10.0 (n=60), p=0.001	19/30 (63.0%) Vs 18/60 (30.0%), p<0.001	-	-	-	28/30 (93.0%) Vs 32/60 (53%), p<0.001	-	-	-	No difference	-	-	-	-	7/30 (23.0%)Vs 30/60 (50.0), p<0.001
Di Paolo *et al*[39], 2012	169±32.0 (n=154) Vs 149±22.0 (n=62), p=0.001	90.2±6.9 (n=154) Vs 99.5±9.3 (n=62), p<0.001	390±20.0 (n=154) Vs 390±50.0 (n=62)	-	-	48.6±12.1 (n=154) Vs 34.1±8.9 (n=62), p=0.01. Maximum: 94.0 (n=154) Vs 63.0 (n=62)	137/154 (89.0%) Vs 26/62 (42.0%), p<0.001	14/154 (9.0%) Vs 2/62 (3.0%)	-	-	140/154 (91.0%) vs 35/62 (56.0%), p<0.001	-	29/154 (19.0%) vs 8/62 (13.0%)	11/154 (7.0%) vs 10/62 (16.0%)	Deep: 22/154 (14.3%) vs 2/62 (3.2%), p<0.05	39/154 (25.3%) vs 5/62 (8.1%), p<0.008	94/154 (61.0%)vs 37/62 (60.0%)	-	22/154 (14.0%) vs 2/62 (3.0%), p=0.003	49/154 (32.0%)vs 24/62 (39.0%)
Galanti *et al*[40], 2019	-	-	-	-	-	-	-	-	-	-	-	-	-	-	BA > WA, significant	-	-	-	-	-
Malhotra *et*	-	-	-	-	-	-	176/1000 (17.6%) Vs	59/1000	42/1000	39/1000 (3.9%)	636/1000 (63.6%)	5/1000 (0.5%)	-	-	130/1000	-	465/1000	368/1000	-	-

al[41], 2021							256/1000 (25.6%), p<0.0001	(5.9%) Vs 10/1000 (1.0%), p<0.0001	(4.2%) Vs 23/1000 (2.3%), p=0.02	Vs 7/1000 (0.7%), p<0.0001	Vs 484/1000 (48.4%), p<0.0001	Vs 2/1000 (0.2%)			(13.0%) Vs 23/1000 (2.3%), p<0.0001		(46.5%) Vs 454/1000 (45.4%)	(36.8%) Vs 373/1000 (37.3%)		
Moneghetti *et al*[42], 2020	-	-	-	-	-	-	-	-	-	-	-	-	-	-	-	-	-	-	-	-
Pelà *et al*[43], 2015	153±25.0 (n=42) Vs 139±23.0 (n=96), p<0.001	78.0±14.0 (n=42) Vs 81.0±14.0 (n=96)	394±36.0 ms (n=42) Vs 403±34.0 ms (n=96)	-	65.0±29.0 (n=42) Vs 60.0±35.0 (n=96)	41.0±11.0 (n=42) Vs 31.0±11.0 (n=96), p<0.001	29/42 (69.0%) Vs 37/96 (39.0%), p<0.001	5/42 (12.0%) Vs 3/96 (3.0%)	-	-	33/42 (79.0%) Vs 41/96 (43.0%), p<0.001	-	-	-	5/42 (12.0%) Vs 14/96 (15.0%)	-	5/42 (12.0%) Vs 17/96 (18.0%)	-	-	6/42 (14.0%)Vs 41/96 (43.0%), p<0.001
Sheikh *et al*[44], 2013	-	87.0±11.0 (n=329) Vs 94.0±10.0 (n=903), p<0.001	398±23.0 ms (n=329) Vs 403±22.0 ms (n=903), p<0.001	-	-	-	66/329 (20.1%) Vs 291/903 (32.2%), p<0.001	25/329 (7.6%) Vs 33/903 (3.7%), p=0.006	54/329 (16.4%) Vs 74/903 (8.2%), p<0.001	10/329 (3.0%) Vs 4/903 (0.4%), p=0.001	163/329 (49.5%) Vs 182/903 (20.2%), p<0.001	2/329 (0.6%) Vs 0 (0%)	-	0 (0%) Vs 3/903 (0.3%)	75/329 (22.8%) Vs 41/903 (4.5%), p<0.001. Deep: 22/32	-	138/329 (41.9%) Vs 524/903 (58.0%), p<0.001	-	29/329 (8.9%)Vs 23/903 (2.5%), p<0.001	61/329 (18.5%)Vs 164/903 (18.2%)

9 (6.7%) Vs 2/903 (0.2%), p<0.001

Supplementary Table 8 Detailed ST-segment elevation and T-wave inversion (Black vs White), *n* (%)

Ref.	STE	Ascending convex (domed)	Ascending concave	Isoelectric	TWI	TWI (anterior V1, V2)	TWI (anterior beyond V2)	TWI (inferior)	TWI (lateral/ Apical)	TWI (inferolateral/Apical)
Demola *et al*[38], 2019		-	-	-		-	-	-	-	-
Di Paolo *et al*[39], 2012		52/154 (34.0%) vs 1/62 (1.0%), p<0.001	88/154 (57.0%) vs 34/62 (55.0%)	-		V1 to V4: 10/154 (6.5%) Vs -	V5 to V6 & inferior leads: 12/154 (8.0%)	-	-	-
Galanti *et al*[40], 2019		-	-	-		-	V2 to V4: BA > WA, significant	-	-	-
Malhotra *et al*[41], 2021		380/1000 (38.0%) Vs 288/1000 (28.8%), p<0.0001	218/1000 (21.8%) Vs 162/1000 (16.2%), p=0.0017	330/1000 (33.0%) Vs 320/1000 (3.2%)		58/1000 (5.8%) Vs 9/1000 (0.9%), p<0.0001	37/1000 (3.7%) Vs 6/1000 (0.6%), p<0.0001	15/1000 (1.5%) Vs 5/1000 (0.5%), p=0.04	10/1000 (1.0%) Vs 2/1000 (0.2%), p=0.02	9/1000 (0.9%) Vs 1/1000 (0.1%), p=0.02
Moneghetti *et al*[42], 2020		-	-	-		-	-	-	-	-
Pelà *et al*[43], 2015		-	-	-		-	-	-	-	-
Sheikh *et al*[44], 2013		-	-	-		12/329 (3.6%) Vs 21/903 (2.3%)	V1 to V4: 47/329 (14.3%) Vs 23/903 (2.5%), p<0.001	20/329 (6.1%) Vs 15/903 (1.7%), p<0.001	8/329 (2.4%) Vs 3/903 (0.3%), p<0.001	-

Supplementary Table 9 Echocardiographic measurements (Black *vs* White)

Ref.	LVEDD (mm)	Normalized or indexed LVEDD (mm/m²)	LVESD (mm)	Normalized or indexed LVESD (mm/m²)	LVEDV (mL)	LVEDV indexed (mL/m²)	LVESV (mL)	LA volume Index (mL/m²)	SWT or Ventricular septum (mm)	Normalized or indexed ventricular septum (mm/m²)	PWT or posterior free wall (mm)	Normalized or indexed posterior free wall (mm/m²)	RWT	Maximal wall thickness (mm)	LV mass (g)	LV mass/BSA (g/m²)	LV mass/h² (g/m²)	RV diameter (mm)	LA (mm)	RA (mm)	Aortic root (mm)	Mass: Volume	LV sphericity	Absolute & global LV longitudinal strain (%)	Stroke volume index (mL/m²)	E wave (cm/s)	A wave (cm/s)	E/A ratio	h/r ratio	Mitral valve E-wave velocity (m/s)	E′ lateral	E/E′	LVEF (%)
Demola *et al*[38], 2019	46.1±4.2 (n=30) Vs 46.4±4.3 (n=60)	-	28.5±4.0 (n=30) Vs 28.3±3.6 (n=60)	-	100±25.0 (n=30) Vs 97.0±26.0 (n=60)	No difference	32.0±9.0 (n=30) Vs 32.0±11.0 (n=60)	No difference	8.9±1.1 (n=30) Vs 7.8±1.1 (n=60), p<0.0001	-	9.0±1.3 (n=30) Vs 7.9±1.4 (n=60), p<0.0001	-	0.39±0.04 (n=60) Vs 0.34±0.04 (n=60), p<0.0	≥13 mm: 4/154 (x%) Vs 0	175±47.0 (n=30) Vs 149±46.0 (n=60), p=0.0	106±22.0 (n=30) Vs 94.0±18.0 (n=60), p=0.005	43.0±9.0 (n=30) Vs 38.0±7.0 (n=60), p=0.021	-	No difference	-	-	-	-	-	-	-	-	-	-	-	-	-	-

													001		09																		
Di Paolo *et al*[39], 2012	51.0±3.6 (n=154) Vs 51.9±2.6 (n=62)	28.3 ±2.3 (n=154) Vs 28.0 ±1.6 (n=62)	32.7±3.5 (n=154) Vs 33.1±3.3 (n=62)	18.1 ±2.2 (n=154) Vs 17.9 ±1.8 (n=62)	-	-	-	-	9.7±1.3 (n=154) Vs 9.2±1.0 (n=62), p<0.001	5.4±0.8 (n=154) Vs 5.0±0.5 (n=62), p<0.001	9.6±1.4 (n=154) Vs 9.0±0.8 (n=62), p<0.001	5.3±0.8 (n=154) Vs 4.8±0.5 (n=62), p<0.001	-	-	-	101.4±18.7 (n=154) Vs 92.4 ±13.2 (n=62), p<0.001	-	-	35.5±4.5 (n=154) Vs 32.3±2.9 (n=62), p<0.001	-	30.0±3.9 (n=154) Vs 29.2±2.6 (n=62)	-	-	-	-	77.2±13.2 (n=154) Vs 90.1±16.5 (n=62), p<0.001	40.3±9.3 (n=154) Vs 43.1±0.6 (n=62), p<0.03	2.0 ±0.6 (n=154) Vs 2.1 ±0.5 (n=62)	0.38±0.05 (n=154) Vs 0.35±0.03 (n=62), p	-	-	-	65.0±6.0 (n=154) Vs 64.0±5.0 (n=62)

																												< 0.0001					
Galanti *et al*[40], 2019	50.0±0.4 (n=77) Vs 51.0±0.6 (n=53)	-	31.0±0.5 (n=77) Vs 32.0±0.3 (n=53)	-	116±2.0 (n=77) Vs 124±2.0 (n=53), p<0.005	-	41.0±2.8 (n=77) Vs 41.0±0.9 (n=53)	-	10.1±0.1 (n=77) Vs 9.4±0.1 (n=53), p<0.001	-	9.7±0.1 (n=77) Vs 9.2±0.1 (n=53), p<0.001	-	0.39±0.1 (n=77) Vs 0.38±0.2 (n=53)	-	-	99.5±1.7 (n=77) Vs 97.4±1.5 (n=53)	-	22.0±0.2 (n=77) Vs 23.0±1.5 (n=53)	33.0±2.8 (n=77) Vs 32.1±3.0 (n=53)	30.5±1.2 (n=77) Vs 29.8±2.8 (n=53)	-	-	-	GLS: −22.4±0.5 (n=77) Vs −23.4±0.7 (n=53)	-	86.3±2.1 cm (n=77) Vs 85.2±1.5 cm (n=53)	44.4±2.1 cm (n=77) Vs 44.8±0.9 cm (n=53)	1.96±1.0 (n=77) Vs 1.94±1.2 (n=53)	-	-	-	-	66.0±0.4 (n=77) Vs 66.0±0.6 (n=53)
Malhotra *et al*[41], 2021	50.6±4.0 (n=1000) Vs 52.4±3.9	26.6±2.19 (n=1000) Vs 27.9±2.12 (n=1000)	-	-	-	-	-	-	LVWT: 10.1±1.4 (n=1000) Vs 9.15±1.3 (n=1000),	-	-	-	0.38±0.04 (n=1000) Vs 0.36±	-	171±35.0 (n=1000) Vs 168±	89.6±17.5 (n=1000) Vs 88.1±16.5 (n=1000)	-	36.4±4.8 (n=1000) Vs 36.6±4.8 (n=1000)	-	-	27.9±3.26 (n=1000) Vs 27.6±	-	-	-	-	-	-	2.02±0.5 (n=1000) Vs 2.1±0.6	-	-	-	-	-

	(n=1000), p<0.0001	, p<0.0001							p<0.0001				0.05 (n=1000), p<0.0001		33.0 (n=1000), p=0.048	, p=0.04					3.2 (n=1000), p=0.01							(n=1000), p=0.0012					
Moneghetti *et al*[42], 2020	-	29.0±2.0 (n=71) Vs 29.0±2.0 (n=130)	-	-	-	89.0±12.0 (n=71) Vs 93.0±12.0 (n=130), p=0.025	-	21.0±6.0 (n=71) Vs 24.0±6.0 (n=130), p=0.005	-	-	-	-	0.31±0.03 (n=71) Vs 0.29±0.02 (n=130), p<0.001	-	-	81.0±10.0 (n=71) Vs 78.0±11.0 (n=130)	-	-	-	-	-	0.91±0.09 (n=71) Vs 0.83±0.08 (n=130), p<0.001	1.78±0.14 (n=71) Vs 1.81±0.13 (n=130)	Absolute: 18.6±2.0 (n=71) Vs 19.0±2.0 (n=130)	49.0±9.0 (n=71) Vs 53.0±9.0 (n=130), p=0.003	-	-	-	-	0.82±0.18 (n=71) Vs 0.78±0.15 (n=130)	17.0±3.7 (n=71) Vs 16.3±3.2 (n=130)	5.0±1.3 (n=71) Vs 5.0±1.2 (n=130)	58.0±4.0 (n=71) Vs 59.0±4.0 (n=130)
Pelà *et*	45.8±	-	27.8±	-	109±22.0	-	35.0±11.	-	9.8±1.7	-	10.0±1.8	-	0.44±	Maximal	Absol	117±27.0	-	-	-	-	-	-	-	-	-	-	-	-	-	-	-	-	-

al[43], 2015	3.8 (n=42) Vs 47.2±4.5 (n=96), p<0.05		4.1 (n=42) Vs 29.2±4.2 (n=96)		(n=42) Vs 111±24.0 (n=96)		0 (n=42) Vs 37.0±12.0 (n=96)		(n=42) Vs 8.5±1.2 (n=96), p<0.001		(n=42) Vs 8.1±1.2 (n=96), p<0.001		0.07 (n=42) Vs 0.35±0.04 (n=96), p<0.001	: 10.3±1.7 (n=42) Vs 8.8±1.1 (n=96), p<0.001	ute: 194±58.0 (n=42) Vs 164±45.0 (n=96), p<0.001	(n=42) Vs 101±20.0 (n=96), p<0.001																	
Sheikh *et al*[44], 2013	51.4±5.0 (n=329) Vs 51.0±5.1 (n	-	-	-	-	-	-	-	-	-	-	-	0.39±0.07 (n=329) Vs 0.37±0.0	Maximal: 10.0±1.5 (n=329) Vs 9.3±1.2 (n=9	-	98.0±23.5 (n=329) Vs 95.3±21.3 (n=903)	-	-	34.7±4.7 (n=329) Vs 33.8±4.5 (n	-	29.0±3.1 (n=329) Vs 28.8±3.6 (n	-	-	-	-	-	-	2.19±0.78 (n=329) Vs 2.21±0.7	-	-	-	-	-

=903)	6 (n=903), p<0.001	03), p<0.001	=903)	=903), p<0.001	8 (n=903)

Supplementary Table 10 Risk of bias assessment–Electrocardiographic parameters

Ref.	Pre-intervention and at-intervention domains			Post-intervention domains				Overall risk of bias
	Confounding	Measurement of exposure	Selection of participants	Post-exposure interventions	Missing data	Measurement of outcomes	Selection of the reported result	
Demola *et al*[38], 2019	Some concern	High-risk	Low-risk	Low-risk	High-risk	Low-risk	Low-risk	High-risk
Di Paolo *et al*[39], 2012	High-risk	Low-risk	Low-risk	Low-risk	Some concerns	Low-risk	Low-risk	High-risk
Galanti *et al*[40], 2019	High-risk	Low-risk	Low-risk	Low-risk	Some concerns	Low-risk	Low-risk	High-risk
Malhotra *et al*[41], 2021	High-risk	Some concerns	Low-risk	Low-risk	Some concerns	Low-risk	Low-risk	High-risk
Moneghetti *et al*[42], 2020	High-risk	Some concerns	Low-risk	Low-risk	Some concerns	Low-risk	Low-risk	High-risk
Pelà *et al*[43], 2015	High-risk	Some concerns	Low-risk	Low-risk	Some concerns	Low-risk	Low-risk	High-risk
Sheikh *et al*[44], 2013	High-risk	Some concerns	Low-risk	Low-risk	Some concerns	Low-risk	Low-risk	High-risk

Supplementary Table 11 Risk of bias assessment–Echocardiographic parameters

Ref.	Pre-intervention and at-intervention domains			Post-intervention domains				Overall risk of bias
	Confounding	Measurement of exposure	Selection of participants	Post-exposure interventions	Missing data	Measurement of outcomes	Selection of the reported result	
Demola *et al*[38], 2019	Some concern	High-risk	Low-risk	Low-risk	High-risk	Low-risk	Low-risk	High-risk
Di Paolo *et al*[39], 2012	High-risk	Low-risk	Low-risk	Low-risk	Some concerns	Low-risk	Low-risk	High-risk
Galanti *et al*[40], 2019	High-risk	Low-risk	Low-risk	Low-risk	Some concerns	Low-risk	Low-risk	High-risk
Malhotra *et al*[41], 2021	High-risk	Some concerns	Low-risk	Low-risk	Some concerns	Low-risk	Low-risk	High-risk
Moneghetti *et al*[42], 2020	High-risk	Some concerns	Low-risk	Low-risk	Some concerns	Low-risk	Low-risk	High-risk
Pelà *et al*[43], 2015	High-risk	Some concerns	Low-risk	Low-risk	Some concerns	Low-risk	Low-risk	High-risk
Sheikh *et al*[44], 2013	High-risk	Some concerns	Low-risk	Low-risk	Some concerns	Low-risk	Low-risk	High-risk